REPORT DOCUMENTATION PAGE

Form Approved
OMB No. 0704-0188

1. REPORT DATE *(DD-MM-YYYY)* 09/09/2010	**2. REPORT TYPE** Final technical	**3. DATES COVERED** *(From - To)* 07/15/2009-05/31/2010

4. TITLE AND SUBTITLE A NEW EDDY-BASED MODEL FOR WALL-BOUNDED TURBULENT FLOWS	**5a. CONTRACT NUMBER** **5b. GRANT NUMBER** FA9550-09-1-0569 **5c. PROGRAM ELEMENT NUMBER**
6. AUTHOR(S) Alexander J. Smits	**5d. PROJECT NUMBER** **5e. TASK NUMBER** **5f. WORK UNIT NUMBER**
7. PERFORMING ORGANIZATION NAME(S) AND ADDRESS(ES) Princeton University Nassaue Street, Princeton NJ 08544	**8. PERFORMING ORGANIZATION REPORT NUMBER**
9. SPONSORING / MONITORING AGENCY NAME(S) AND ADDRESS(ES) AFOSR Dr. John Schmisseur - NA 875 North Randolph Street, Suite 325, Room 3112, Arlington, Virginia 22203	**10. SPONSOR/MONITOR'S ACRONYM(S)** **11. SPONSOR/MONITOR'S REPORT NUMBER(S)** AFRL-OSR-VA-TR-2012-0728

12. DISTRIBUTION / AVAILABILITY STATEMENT

Suitable for Public Release

13. SUPPLEMENTARY NOTES

14. ABSTRACT

We have completed preliminary work to develop a new model for turbulent wall-bounded flows that captures the correct scaling behavior of the turbulence intensities and other near-wall statistics (including skin friction) for a wide range of Reynolds numbers. Such information can be used for prediction purposes and may be the basis of a new approach to the near-wall model problem in Large Eddy Simulation (LES). The model is based on our new understanding of turbulent structure in subsonic, supersonic and hypersonic flows. We use the concept of the attached eddy hypothesis to map the attributes of each eddy type in physical space to wavenumber space. Experimental data are then used to determine the scaling behavior of the basic eddy motions in wavenumber space, and the scaling behavior of the Reynolds stress behavior is recovered by integrating over all wavenumbers.

15. SUBJECT TERMS

Turbulence, aerodynamics,

16. SECURITY CLASSIFICATION OF:			**17. LIMITATION OF ABSTRACT**	**18. NUMBER OF PAGES**	**19a. NAME OF RESPONSIBLE PERSON**
					Alexander J. Smits
a. REPORT	**b. ABSTRACT**	**c. THIS PAGE**	UU	24	**19b. TELEPHONE NUMBER** *(include area code)*
U	U	U			(609) 258 5117

Final Technical Report
FA9550-09-1-0569
submitted to the
Air Force Office of Scientific Research

ATTN: Dr. John Schmisseur - NA 875
North Randolph Street, Suite 325, Room 3112, Arlington, Virginia 22203
Tel: (703) 696-6962; Fax: (703) 696-8451
E-mail: john.schmisseur@afosr.af.mil

Submitted by

Princeton University
Princeton, New Jersey 08544, U.S.A.

A NEW EDDY-BASED MODEL FOR WALL-BOUNDED TURBULENT FLOWS

Grant FA9550-09-1-0569
For the period July 15, 2009 May 31, 2010

Alexander J. Smits, Principal Investigator
Department of Mechanical and Aerospace Engineering
Princeton University, Princeton, NJ 08544
Email: asmits@princeton.edu
Phone: 609 258 5117; Fax: 609 258 1918

A NEW EDDY-BASED MODEL FOR WALL-BOUNDED TURBULENT FLOWS

Final Technical Report

ABSTRACT

We have completed preliminary work to develop a new model for turbulent wall-bounded flows that captures the correct scaling behavior of the turbulence intensities and other near-wall statistics (including skin friction) for a wide range of Reynolds numbers. Such information can be used for prediction purposes and may be the basis of a new approach to the near-wall model problem in Large Eddy Simulation (LES).

The model is based on our new understanding of turbulent structure in subsonic, supersonic and hypersonic flows. Specifically, we identify four basic eddy motions: (1) the streaks associated with longitudinal vortex-like structures in the near-wall region, as identified by Kline et al. (1967); (2) the hairpin or horseshoe vortices first described by Theodorsen (1952); (3) the Large-Scale Motions (LSMs) which are related to the groups of horseshoe vortices or "vortex packets" defined by Head & Bandyopadhyay (1981) and Adrian et al. (2000); and (4) the Very Large-Scale Motions (VLSMs) interpreted by Liu et al. (2001) in terms of the outer layer bulges and by Monty et al. (2007) in terms of the meandering superstructures observed in pipe, channel and boundary layers.

We use the concept of the attached eddy hypothesis to map the attributes of each eddy type in physical space to wavenumber space. Experimental data are then used to determine the scaling behavior of the basic eddy motions in wavenumber space, and the scaling behavior of the Reynolds stress behavior is recovered by integrating over all wavenumbers.

1. STATEMENT OF OBJECTIVES

We report the preliminary results of a combined experimental/theoretical program to study the behavior of wall-bounded turbulent flows over a very large Reynolds number range. The aim is to develop a new model for the turbulence behavior that is based on our knowledge of the coherent structures observed in such flows. The approach taken here is to build on the attached eddy model originally proposed by Townsend (1976) and refined by Perry & Chong (1982), Perry, Henbest & Chong (1986), Fernando & Smits (1988), Perry & Marusic (1995), and Marusic, Uddin & Perry (1997).

The attached eddy model describes turbulence in wall-bounded flows as consisting of a superposition of a number of distinct classes of eddies, where the different classes correspond to the coherent structures observed in experiment. The eddies are scaled into hierarchies, and each hierarchy has the correct scaling and statistical properties so that the ensemble of hierarchies reproduces both the mean flow, and the spectral behavior of the turbulence. The most important aspect of the attached eddy model is the underlying scaling argument that anchors the model to a firm physical foundation. Because the model is based on eddy physics derived from observations of turbulent structure, it is expected to be more robust to changes in boundary conditions than traditional models used in Reynolds-Averaged Navier-Stokes solvers. Here, we build on this foundation to define eddy functions that capture the contributions of the principal coherent motions to the turbulence energy and shearing stress in wavenumber space. Preliminary results (Smits, 2010) have demonstrated the remarkable result that only three eddy functions, corresponding to the large-scale motions, very large-scale motions, and the motions responsible for the near-wall energy production, are sufficient to capture the spectral behavior of wall-bounded turbulence, and, by integration, predict the turbulence intensity distribution in boundary layers over a very large Reynolds number range.

The existing attached eddy model has had some notable successes, such as the derivation of scaling laws for the three components of turbulence, and the successful scaling of the streamwise component of the turbulence for Reynolds numbers corresponding to small laboratory facilities all the way to atmospheric boundary layers (Marusic & Kunkel, 2003). It was extended to compressible flows, at least at an elementary level, by Fernando & Smits (1988), Dussauge & Smits (1995) and Smits & Dussauge (2006). This work has established the attached eddy model as the preferred interpretation for the structure of turbulence, and the primary basis for understanding the interaction among different scales of motion. We now need to test its full capability by expanding the model scope so that it will reproduce many other features of flat plate boundary layers, such as the spectral distribution of scales, higher order moments, and components of turbulence other than the streamwise stress, in particular the shear stress distribution. In addition, we now know that turbulent boundary layers and other wall-bounded flows such as pipe or channel flows display previously unsuspected differences that have not yet been incorporated in the attached eddy model. Furthermore, the model needs to include the effects of pressure gradient, wall curvature, and heat transfer. Finally, incorporating density variations and compressibility is still at a rudimentary stage, and there have not yet been any serious attempt to develop the attached eddy model to describe the behavior of supersonic and hypersonic turbulent boundary layers.

In the following, we describe the current state of the art in the attached eddy model in more detail, and summarize our progress in expanding the model to incorporate more detailed flow physics based on a wavelet interpretation of eddy structure.

2. RESEARCH EFFORT

2.1 The Structure of Turbulence

In considering the structure and scaling of wall turbulence at high Reynolds numbers we start with the "classical" position where the boundary layer is held to be composed of two principal regions that follow distinct scalings: a near-wall region where viscosity is important, and the outer region where it is not. On the basis of the mean momentum equation, the velocity and length scales in the near wall region are taken to be $u_\tau = \sqrt{\tau_w/\rho}$ and ν/u_τ, respectively, where τ_w is the wall stress, ρ is the fluid density, and ν is the fluid kinematic viscosity. In the outer region, it is assumed that the appropriate length scale is the boundary layer thickness δ, or a scale related to δ, and the velocity scale continues to be u_τ, since u_τ sets up the inner boundary condition for the outer flow.

As to the structure of turbulence, in the current view we identify four principal characteristic elements (Smits *et al.*, 2011). The first two, near-wall streaks with a typical spanwise spacing of about $100\nu_w/u_\tau$ (Kline *et al.*, 1967), and hairpin or horseshoe vortices with a range of scales starting with a minimum height of $100\nu_w/u_\tau$ (Theodorsen, 1952), have been recognized for a long time. More recently, visualizations, numerical studies and experiments on wall-flows have revealed the existence of two new elements, the so-called large- and very large-scale motions.

Large-Scale Motions (LSM) are believed to be created by the vortex packets formed when multiple hairpin structures travel at the same convective velocity (Zhou *et al.* 1999, Kim & Adrian 1999, Guala *et al.* 2006, Balakumar & Adrian 2007). They are related to the features first seen by Head & Bandyopadhyay (1981) that consisted of hairpins with their heads inclined at approximately 20° to the wall, but what has become clear, especially through the work of Adrian *et al.* (2000), is that these features are far more common and important than Head & Bandyopadhyay realized at the time. A characteristic feature of the LSM is that the hairpin vortices within the packet align in the streamwise direction and induce regions of low streamwise momentum between their legs (Adrian *et al.*, 2000; Brown & Thomas, 1977; Ganapathisubramani *et al.*, 2003; Hutchins *et al.*, 2005; Tomkins & Adrian, 2003). The LSM have a streamwise scale of approximately 2-3δ and have been associated with the occurrence of bulges of turbulent fluid at the edge of the wall layer, where δ is the boundary layer thickness. A thorough review of the evidence supporting the existence of hairpin vortices and their organization into packets is provided by Adrian (2007).

In addition to the LSM, very long, meandering, features consisting of narrow regions of low streamwise momentum fluid flanked by regions of higher momentum fluid have been observed in the logarithmic and wake regions of wall-flows (Balakumar & Adrian, 2007; Guala *et al.*, 2006; Hutchins & Marusic, 2007*b*; Kim & Adrian, 1999; Monty *et al.*, 2007; Tomkins & Adrian, 2005). In internal flows, the motions are typically referred to as Very-Large-Scale Motions (VLSM), whereas in external flows they are more commonly referred to as "superstructures." Both VLSM and superstructures appear to scale on outer variables, and although the spanwise/azimuthal meandering of these regions makes it difficult to determine their typical streamwise extent, hot-wire rake measurements in channels and pipes (Monty *et al.*, 2007) have found instances of VLSM in internal flows as long as 30 times the channel half-height h or pipe radius R, while similar experiments in boundary layers (Hutchins & Marusic, 2007*b*) show instances of superstructures with lengths up to 10-15 times the boundary layer thickness. These lengths are typically shorter when inferred from single-point frequency spectra ($\sim$10-20R for pipes and $\sim 6\delta$ for boundary layers). In addition, Monty *et al.* (2009) note that the superstructures in boundary layers appear to be limited to the logarithmic region, whereas for internal geometries the VLSM are found to persist well into the outer layer (Bailey & Smits, 2010). In contrast, Tutkun *et al.* (2009) found evidence of weak elongated structures within boundary layers out to the edge of the layer.

Spectral analysis of the VLSM and LSM indicates that they make a significant contribution to the turbulent kinetic energy and Reynolds stress production (Balakumar & Adrian, 2007; Guala *et al.*, 2006), which distinguishes them from the inactive motions proposed by Townsend (1976). For example, Balakumar & Adrian (2007) found that 40-65% of the kinetic energy and 30-50% of the Reynolds shear stress is accounted for in the long modes with streamwise wavelengths $\lambda_x/\delta > 3$. Similar estimates for the contribution to the Reynolds shear stress from vortex packet structures were made by Ganapathisubramani *et al.* (2003), who used a feature-detection algorithm on stereoscopic PIV data in streamwise-spanwise planes in the log layer. Careful analysis of DNS data has also revealed the footprint of the outer-scaled motions within the inner-scaled inner layer (Abe *et al.*, 2004; Hoyas & Jiménez, 2006; Hutchins & Marusic, 2007*a*,*b*), and Mathis *et al.* (2009) found modulation of the near wall cycle by long wavelength motions further from the wall, which is supported by the correlations measured by Tutkun *et al.* (2009) and the recent simulation results by Schlatter *et al.* (2009). These results suggest that motions in the logarithmic and outer layer may have a strong influence on the behavior of the near wall turbulence. This is a significant observation in that it suggests a new approach for developing near-wall models for LES, a topic that we will explore as an important part of our future work.

2.2 The Attached Eddy Model

Here we give a description of the attached eddy model, and how the observations on coherent motions are incorporated in the model. The model essentially provides a kinematic description for wall-bounded turbulence. The foundation of the model, which is based on the attached-eddy hypothesis of Townsend (1976), is the observation that wall-bounded turbulence contains a collection of coherent structures or eddies. Therefore, the model proposes that the statistical features of wall-bounded turbulence can be modelled by a linear superposition of such eddies. The model has been refined and developed over the past three decades on the data of low-to-moderate Reynolds number wall-bounded turbulence experiments (e.g. pipe and boundary-layer flow) and has led to a number of similarity laws. For a complete review of the attached-eddy model see Perry & Marusic (1995) and the references therein.

One of the strengths of the attached-eddy model is the physical framework it provides for the analysis and understanding of the mechanism of wall-bounded turbulence. For example, Perry & Abell (1975), Perry, Henbest & Chong (1986), and Perry & Li (1990) used this framework along with simple dimensional-analysis arguments applied to the velocity contributions of the attached eddies to suggest several regions of spectral scaling. They assumed that a turbulent boundary layer outside the viscous region may be modeled as a forest of hairpin or Λ-shaped vortices, which originate at the wall and grow outward. Figure 1 shows three Λ-shaped vortices of different scales, and indicates their influence on the velocity field sensed by a probe at a position y. The probe will sense contributions to u' and w' from all eddies of scale y and larger. However, only eddies of scale y will contribute to v'. Therefore, u' and w' should follow similar scaling laws, whereas v' is expected to follow a somewhat different scaling law. Using these ideas in conjunction with dimensional analysis, scaling laws can be derived for the energy spectra in the turbulent wall region, defined as $\nu/u_\tau \ll y \ll \delta$ (Perry et al., 1986). In general, it is the region where it is assumed that direct wall effects such as the damping of the velocity components are unimportant, and where the direct influence of the large-scale flow geometry and outer boundary conditions can also be neglected. This region corresponds approximately to the overlap region in the mean velocity profile, that is, the region where the velocity has a logarithmic variation.

For the u'-component of the turbulence fluctuations in an incompressible flow, it is argued that eddies of scale δ will contribute only to the large-scale, low wavenumber (low frequency) region of the energy spectrum Φ_{11}. For the large-scale eddies, viscosity is not important, and the spectrum in the low wavenumber region should depend only on u_τ, k_1, y, and δ, where k_1 is the streamwise component of the three-dimensional wavenumber vector $\mathbf{k}$. Eddies of scale y (the attached eddies) will contribute to the intermediate wavenumber range of the spectrum, whereas eddies of scale δ will not. The smallest scale motions, which contribute to the high wavenumber range of the spectrum, depend on viscosity. Kolmogorov (1941) assumed that these small-scale motions are locally isotropic, and that their energy content depends only on the local rate of turbulence energy dissipation ε, and the kinematic viscosity ν, so that their characteristic length scale is $\eta = (\nu^3/\varepsilon)^{1/4}$.

Just as the mean flow exhibits an inner and outer scaling with a region

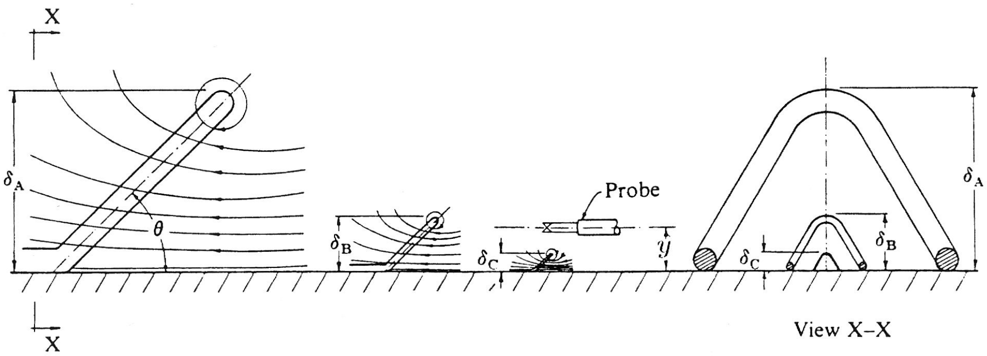

Figure 1: Sketch of the streamline patterns and spatial influence of attached eddies at three different scales. From Perry *et al.* (1986).

of overlap, it is expected that there will be an overlap region in wavenumber space between the δ-sized motions and the y-sized motions. Dimensional analysis then indicates that, in this overlap region, the spectrum follows a k^{-1} scaling. We also expect that there will be an overlap region in wavenumber space between the y-sized motions and the η-sized motions. This leads to a spectrum following a $k^{-5/3}$ scaling.

By integrating these spectral forms, Perry & Li (1990) derived the following expressions for the normal stresses in a subsonic boundary layer:

$$\frac{\overline{u'^2}}{u_\tau^2} = B_1 - A_1 \ln\left(\frac{y}{\delta}\right) - V(y^+), \tag{1}$$

$$\frac{\overline{w'^2}}{u_\tau^2} = B_3 - A_3 \ln\left(\frac{y}{\delta}\right) - V(y^+), \tag{2}$$

$$\frac{\overline{v'^2}}{u_\tau^2} = A_2 - V(y^+), \tag{3}$$

where B_1 and B_2 are large-scale characteristic constants, particular to the flow geometry, and A_1, A_2, and A_3 are expected to be universal constants (all the constants are positive). The logarithmic term comes from the k^{-1} portion of the spectrum. The function $V(y^+)$ comes from the inertial ($k^{-5/3}$ plus dissipation) portion of the spectrum, and it is a Reynolds number dependent, viscous correction term that increases with y^+. Note that equations 1 to 3 are valid only in the turbulent wall region.

These turbulence intensity similarity formulations, and the spectral similarity arguments on which they are based, have been tested for a variety of wall-bounded flows and the results used to further improve the model. For instance, the suggested formulations have been investigated using smooth-pipe flow (Perry et al. 1986), smooth and rough zero-pressure-gradient turbulent boundary layers (Perry & Li 1990), and favorable- and adverse-pressure-gradient turbulent boundary layers (Jones, Marusic & Perry 2001 and Marusic & Perry 1995, respectively).

Marusic *et al.* (1997) extended these scaling laws to include the entire region outside the viscous sublayer (the original formulations were only valid in the log region). As with the mean flow, the deviation from the logarithmic profile near the wall is attributed to viscous effects, and the deviation in the outer part of the layer is due to wake effects. They suggested a "wall-wake" distribution where, for example,

$$\frac{\overline{u'^2}}{u_\tau^2} = B_1 - A_1 \ln\left(\frac{y}{\delta}\right) - V_{g1}(y^+) - W_{g1}\left(\frac{y}{\delta}\right). \tag{4}$$

They called V_{g1} the *viscous deviation* (actually a more complete version of function V in equation 1), and W_{g1} the *wake deviation.* Marusic et al. (1997) gave empirical forms for V_{g1} and W_{g1} that agreed well with data over the range $6570 \leq Re_\theta \leq 35100$. An extension of Equation 4 that applies across the entire boundary layer including the viscous near-wall layer was proposed by Marusic & Kunkel (2003), and comparisons with the laboratory data of DeGraaff & Eaton (2000) and the atmospheric data of Metzger & Klewicki (2001) showed excellent agreement (Figure 2), although the formulation does not reproduce the outer peak in the streamwise intensity observed at high Reynolds numbers seen by Fernholz et al. (1995), and Morrison et al. (2004). A similar high level of agreement with high Reynolds number pipe flow data was shown by Marusic *et al.* (2004).

Despite its apparent success, there are a number of compelling reasons to revisit this model. First, the model is based on the presence of k^{-1} and $k^{-5/3}$ regions in the spectrum. Although the $k^{-5/3}$ is well established, experiments now indicate that the k^{-1} region is only evident at very high Reynolds numbers over a very limited spatial extent (see, for example, Morrison et al. 2004, and Nickels et al. 2005). Second, the interactions between outer layer motions and inner layer motions have become much clearer in recent years, and the simple division between inner and outer layer scaling that

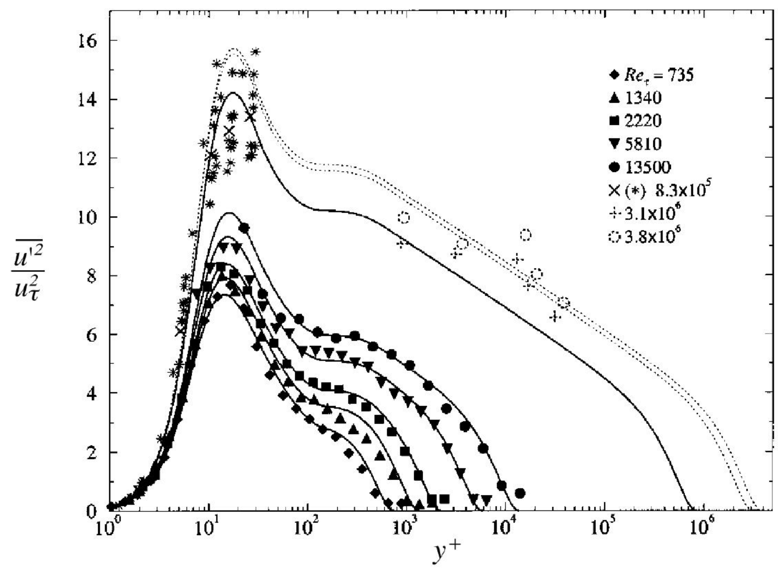

Figure 2: Streamwise turbulence intensity measurements: high Reynolds numbers from ASL (Metzger & Klewicki; Marusic et al.); low Reynolds number data from DeGraaff & Eaton (2000). Lines are model results from Marusic & Kunkel (2003).

leads to the k^{-1} region fails to capture that interaction. Specifically, the region where we might expect k^{-1} scaling corresponds to the wavenumbers occupied by the LSMs, and experiments have clearly shown that although the LSMs appear to behave as attached motions, they do not scale simply as y^{-1}. Third, the importance of the VLSMs was not appreciated until recently. For example, the low wavenumber VLSMs contribute about half of the total energy content of the streamwise turbulence component at high Reynolds numbers. Fourth, it has become clear that the relative importance of LSMs, VLSMs, and superstructures depends on the nature of the flow: they behave differently in pipes, channels and boundary layers (Monty et al. 2007, Bailey et al. 2008), something that is not captured in the original model. Fifth, the original model does not include the effects of pressure gradient (although some steps were taken by Perry, Marusic & Jones 2002), compressibility, or heat transfer.

As to the effects of compressibility, recent results at Princeton on the behavior of hypersonic boundary layers have given new confidence that such flows can be incorporated in the attached eddy approach. We have demon-

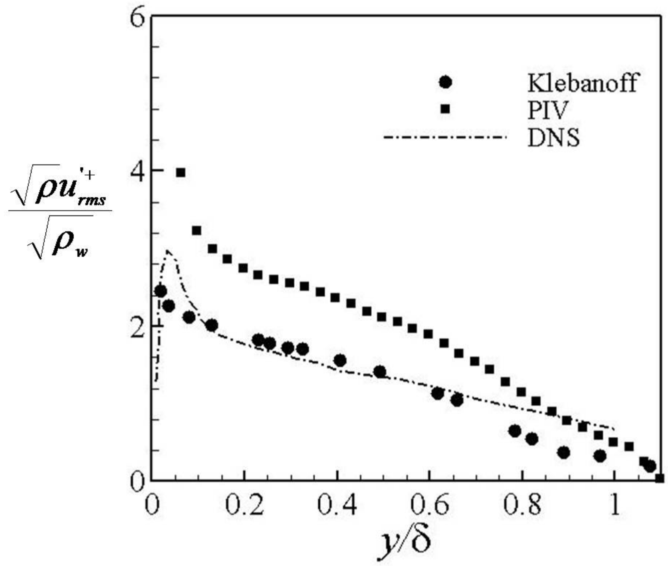

Figure 3: Intensity of the streamwise component of the velocity fluctuation in a Mach 7.2 turbulent boundary layer using Morkovin scaling ($Re_\tau = 300$, $Re_\theta = 3500$). PIV data from Sahoo *et al.* (2010*a*), DNS from Duan *et al.* (2010).

strated that the mean velocity profile for smooth and rough surfaces, when scaled according to van Driest, follows the incompressible scaling closely (Sahoo *et al.*, 2010*b*, 2009). In addition, the experimental data of Sahoo *et al.* (2010*a*) and the DNS results by Duan *et al.* (2010) have provided the first clear evidence that Morkovin's scaling continues to apply up to Mach numbers of 7.2 (see Figure 3). These results validate the approach taken by Fernando & Smits (1988) in extending the attached eddy hypothesis to compressible boundary layers, and Dussauge & Smits (1995) in extending the scaling arguments underlying equation 1 to high speed flows. Taken as a whole, this work opens up a clear path to generalizing the incompressible model to high Mach numbers.

2.3 Technical Approach and Results

To overcome the limitations of the existing model described above, we have conducted a combined theoretical and experimental study to develop a new model that captures the correct spectral behavior of wall-bounded turbulence, and allows prediction of Reynolds stress distributions in general wall-

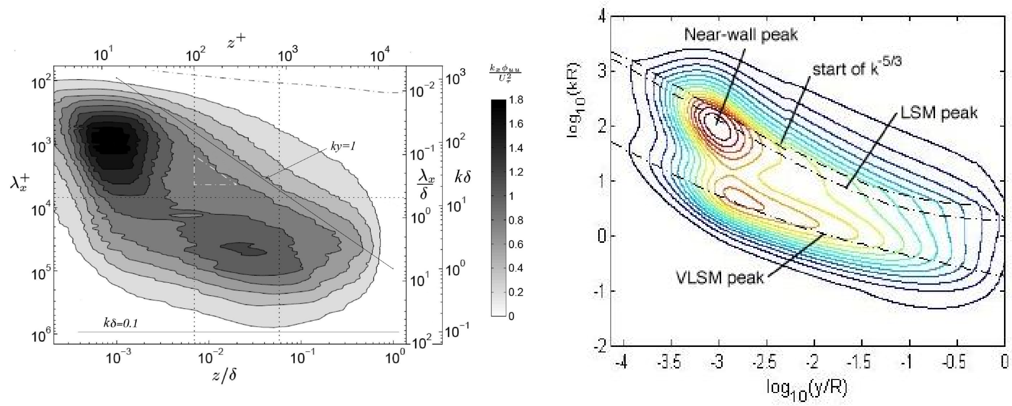

Figure 4: Contour maps of pre-multiplied spectra for the streamwise component of the velocity fluctuation in a zero pressure gradient turbulent boundary layer for $Re_\tau = 14$K. Left: data from Hutchins & Marusic (2007*b*); right: model predictions.

bounded flows.

A preliminary form for the new model has now been established (Smits, 2010). Here, the four basic eddy motions are modeled using Gaussian distributions in the log of the wave number. This represents a more complete formulation, when compared to the Perry et al. model, in the sense that the full wavenumber distributions are specified, instead of just noting regions of k^{-1} and $k^{-5/3}$ scaling. The energy contained at each wavenumber is taken to be a simple sum over all eddy types, neglecting nonlinear interactions among eddies. The high wavenumber part of the spectrum is bounded by the $k^{-5/3}$ inertial and dissipation ranges, which are modeled as a single cutoff using a modified Pao spectrum. The results are compared with the data of (Hutchins & Marusic, 2007*b*) in figure 4, which show the contour maps of pre-multiplied spectra for the streamwise component of the velocity fluctuation in a zero pressure gradient turbulent boundary layer. The predictions for the turbulence intensity for three different Reynolds numbers are given in figure 5, which shows that even at this preliminary stage the new model performs as well as the original model shown in figure 2 while capturing the actual spectral behavior much more closely.

The results are remarkable in that only three eddy functions are sufficient to capture the spectral behavior of wall-bounded turbulence, and, by integration, predict the turbulence intensity distribution in boundary layers over a very large Reynolds number range. The model shown in figure 4 uses sim-

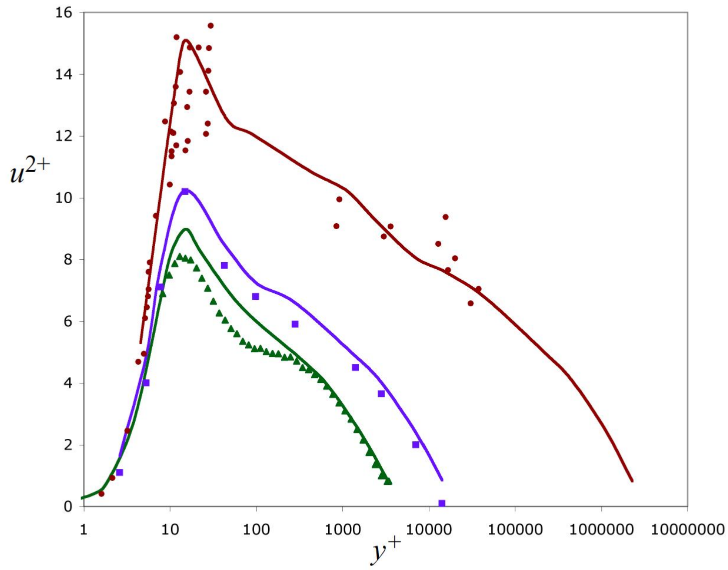

Figure 5: Intensity of the streamwise component of the velocity fluctuation. Data points from Bailey (pipe, $Re_\tau = 3.3\text{K}$), DeGraaff (boundary layer, $Re_\tau = 14\text{K}$), and Kunkel (boundary layer, $Re_\tau = 2.3\text{M}$), respectively. Lines are model predictions at the same Reynolds numbers.

ple Gaussian distributions in log-wavenumber space to represent the energy content of the three basic eddy structures (near-wall streaks, hairpin vortices arranged in packets to form LSMs, and VLSMs/superstructures), and empirically determined functions are used to control the scaling of these energy distributions in physical and wavenumber space. The log-wavenumber distributions used here have some attractive properties (they are analytically integrable, for example), but we need to develop eddy functions that have a more physical basis. We are attracted to the concept of wavelet-based eddy functions, primarily because wavelets appear to represent well the characteristic velocity signatures seen in turbulence. For example, Tennekes & Lumley (1972) proposed the concept of a "simple eddy" as a possible model for the coherent motions in turbulent flows, and the simple eddy they suggested is well-represented by a Mexican Hat wavelet function in physical space, as we shall see.

Some guidance on the use of wavelets to build eddy functions can be found in recent experimental results from the Princeton University Superpipe

(Bailey & Smits, 2010). These experiments used filtered cross-correlations of multi-probe hot-wire data to elucidate more information about the structure of LSMs and VLSMs. These filtered cross-correlations, samples of which are shown in figure 7, suggest that these motions could be modeled using simple wavelet eddy models. Figure 7 indicates that the form of wavelet best representing each type of motion varies, with VLSMs represented using

$$g(t) = \frac{t}{a} e^{-(t/\sqrt{2}a)^2} \tag{5}$$

and LSMs represented using a *Mexican Hat* wavelet such as

$$g(t) = \left(1 - \frac{t}{a}\right)^2 e^{-(t/\sqrt{2}a)^2}. \tag{6}$$

where a is a scaling value.

These functions can be considered the real part of a complex function, $g(t)$, whose Fourier transforms are given by

$$G(\omega) = j(a\omega)e^{-(a\omega)^2/2} \tag{7}$$

and

$$G(\omega) = \begin{cases} 2(a\omega)^2 e^{-(a\omega)^2/2} & \text{for} \quad \omega > 0 \\ 0 & \text{for} \quad \omega \leq 0 \end{cases} \tag{8}$$

The wavelet functions $g(t)$ are shown in figure 6 multiplied by a weighting function $w(a)$ used to ensure that the energy of the wavelet is the same at all scales. Also shown in figure 6 are the modulus of the corresponding Fourier transforms. These representations illustrate the localized nature of the wavelet function in both physical and frequency space.

The Fourier transform of these functions were used to model the eddy functions instead of the original Gaussian distributions. As shown in figure 8, the eddy distribution representing the VLSM/superstructure contribution was very successfully modeled by the wavelet function of equation 5, and actually eliminated the need for one of the empirical functions used to define the original Gaussian distribution of energy.

However, our attempts at modeling the LSM contribution using a single wavelet function were less successful. As shown in figure 9a-b, a single wavelet does not incorporate energy across a large enough wavenumber range to model the energy content of the LSMs in a simple way. Note in particular

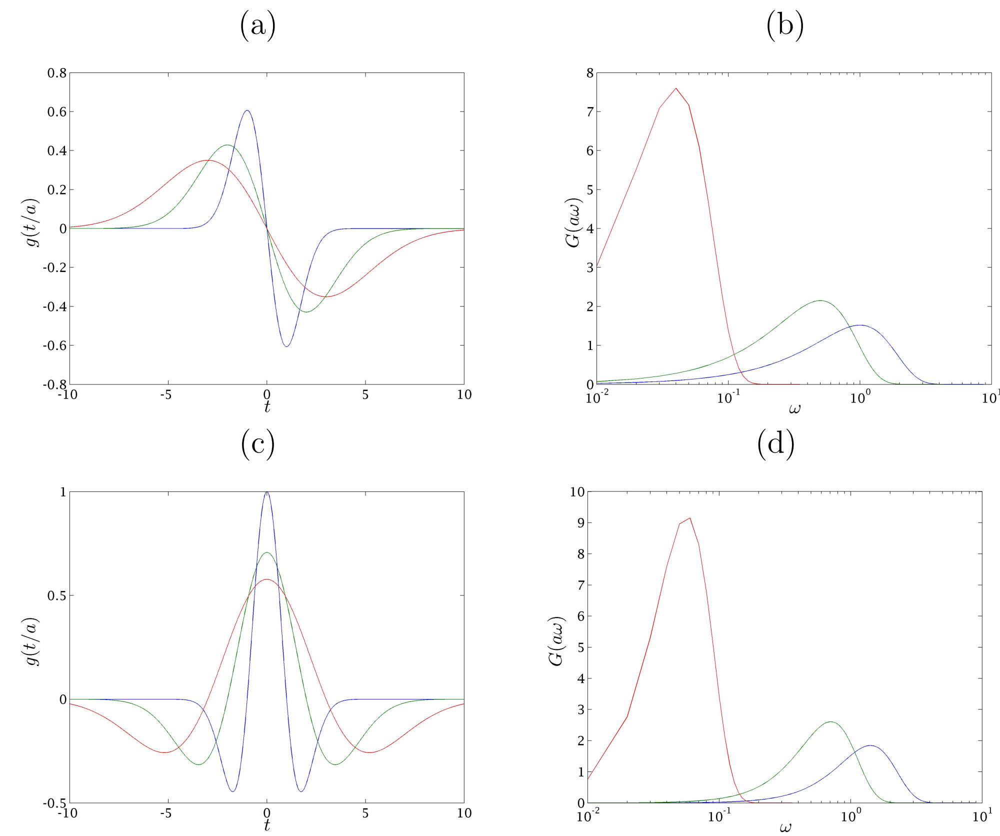

Figure 6: Representative wavelet function for three different scale factors a and $w(a) = 1/\sqrt{a}$: (a) equation 5 in physical space (b) equation 5 in frequency space (c) Mexican Hat in physical space and (d) Mexican Hat in frequency space.

that the Fourier transform of the Mexican Hat wavelet function is Gaussian in the wavenumber, not the log of the wavenumber, so that the eddy functions used in future attempts to model the spectral behavior of the eddies may need to be modified accordingly. Alternatively, this obstacle can be overcome if we model the LSMs as a hierarchy of eddies of containing different wavenumbers, as is done with the Perry et al. model. A simple demonstration is provided in figure 9c where the probability density function of the eddy scales is modeled using a Gaussian distribution. These results illustrate that we can increase the wavenumber distribution of the model LSM eddies, but this is done through the introduction of a new parameter which must also be modeled: the probability distribution of eddies, which corresponds (at least in spirit) to the concept of a hierarchy of eddies as used in the refined attached eddy

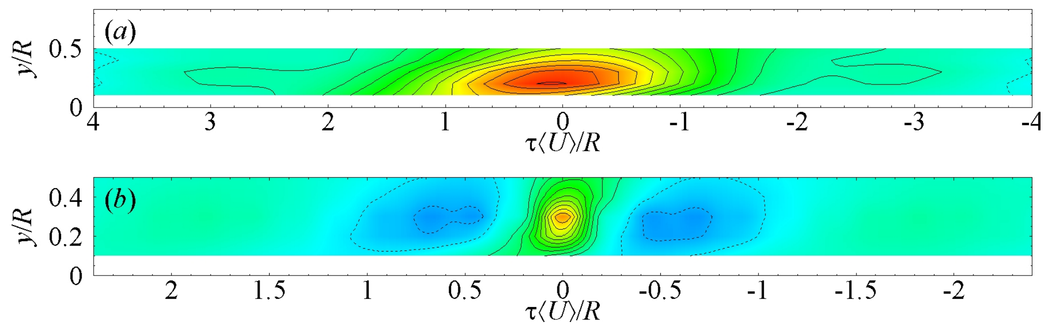

Figure 7: Spectrally filtered cross-correlations with reference probe at different locations from the wall for (a) VLSM wavenumber range and (b) LSM wavenumber range.

hypothesis.

The modeling of the VSLMs (or superstructures), together with the recent finding of Hutchins & Marusic (2007) documenting the interaction of the large-eddy motions on the near wall region, have led to us to propose a new preliminary predictive model for boundary layers. Here, a statistical signature of the full near-wall region can be predicted given only the low-pass filtered velocity signature in the log-region (such as that found in LES). The model is non-linear and is based on a Townsend attached signature together with an amplitude modulation effect. Preliminary tests show the predictive model to be very promising. For example, in figure 10a premultiplied streamwise velocity spectra at $y^+ = 15$ (nominally the location of maximum turbulent energy production) is shown in a high Reynolds number experiment together with a prediction using the new model based on the velocity signature measured at another time in the logarithmic region of the boundary layer. Figure 10b shows the predicted turbulence intensities at $y^+ = 15$ for a range of Reynolds numbers. The model also accurately predicts the increase in skewness and flatness of the streamwise velocity fluctuations with increasing Reynolds number at $y^+ = 15$ (a fact that has been known for some time but never understood).

Although the current work has indicated the potential of this model, there are still several areas which require further exploration:

- What probability distributions can be best used to describe the arrangement of the eddies? These distributions will be a function of both streamwise

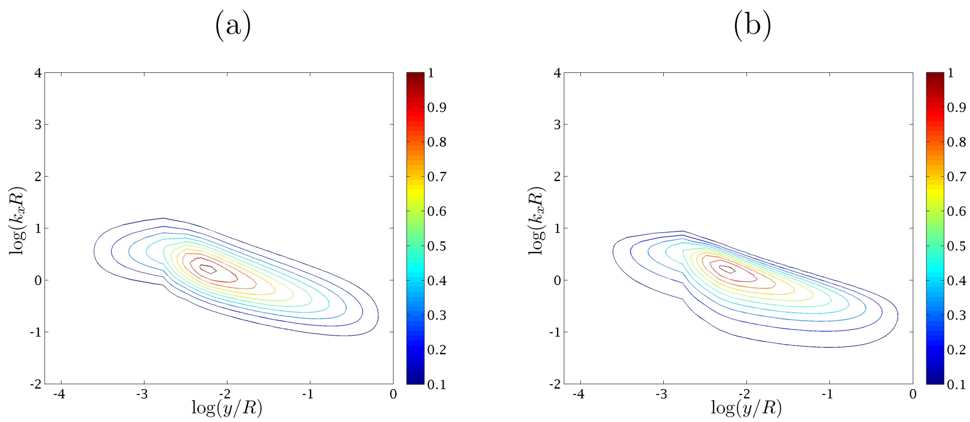

Figure 8: Model energy distribution for VLSMs/superstructures using (a) Gaussian in log-wavenumber space (b) wavelet eddy representation.

and wall-normal wavenumbers and need to be determined from experiment.

- Can we find an analytical description with which to replace the empirical functions used to describe the scaling of the eddy functions?
- Can the differences between the VLSMs and superstructures, and by extension internal and external flows, be accurately captured by a single model or will there be a need for separate models for these different flows?
- It has been suggested that the LSMs and VLSMs are inter-connected. If so, it is possible that the simple linear superposition of energy used in this model could be a poor representation of the physics of their motions. What is the nature of this interaction and can we model it? If this interconnectivity can be determined and incorporated into the model, it could greatly reduce the number of parameters used to describe the eddy functions. Support for this inter-connectivity of the LSMs and VLSMs, along with some suggestions for the nature of their interaction, has been found in the experiments of Bailey & Smits (2010).
- The energy within the near wall streaks has been found to be modulated by the superstructures (Hutchins & Marusic, 2007*b*). Can this interaction be incorporated into the eddy function describing the contribution of the near wall streaks? Can we develop this approach into a new wall function formulation for LES?
- Can the model be expanded to describe the additional Reynolds stress components, especially the shear stress?
- Can the model be expanded to incorporate various effects; that is, wall-

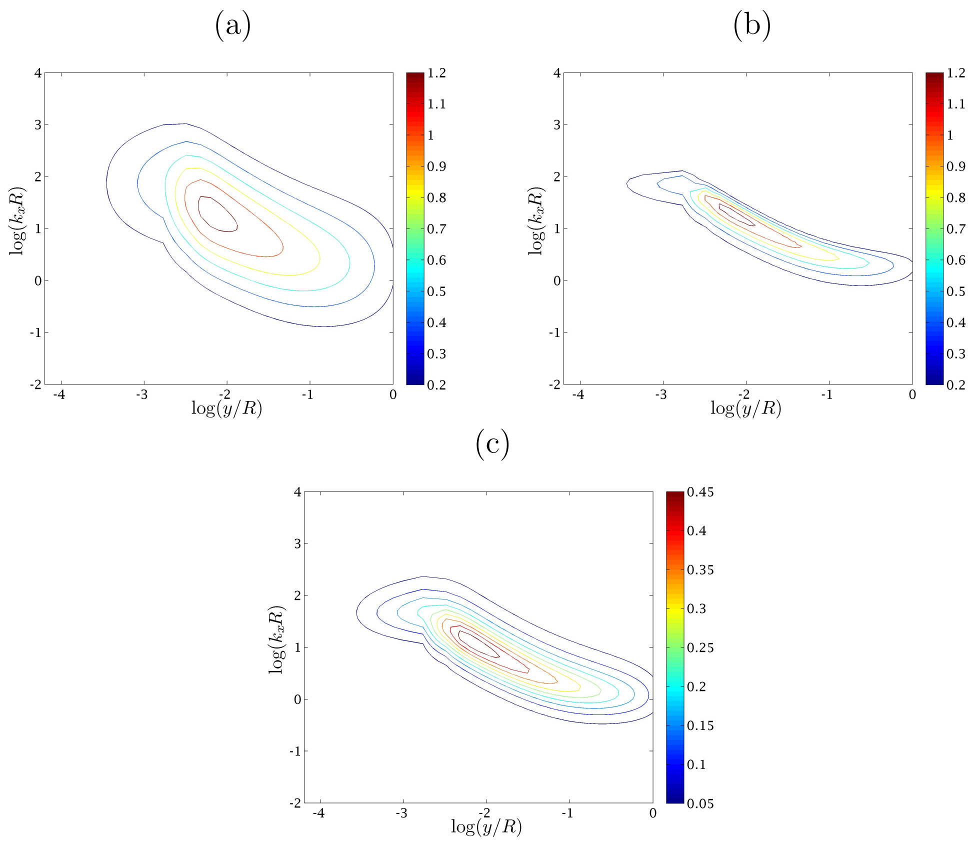

Figure 9: Model energy distribution for LSMs using (a) Gaussian in log-wavenumber space (b) single wavelet eddy representation (c) Gaussian distribution of wavelet model eddies.

roughness, pressure gradients, thermal stability?

2.4 Synergistic Activities

The work was performed jointly by investigators at Princeton University and the University of Melbourne, Australia. The PI has a long history of collaboration with Ivan Marusic, the Melbourne University group headed by Professor Ivan Marusic, as co-organizers of the International Workshops on Wall-Bounded Turbulent Flows (2008, 2006, 2005, 2004, and 2003), co-participants in ICET (International Collaboration on Experiments in Turbulence), and most recently as co-authors (with Beverley McKeon of Caltech)

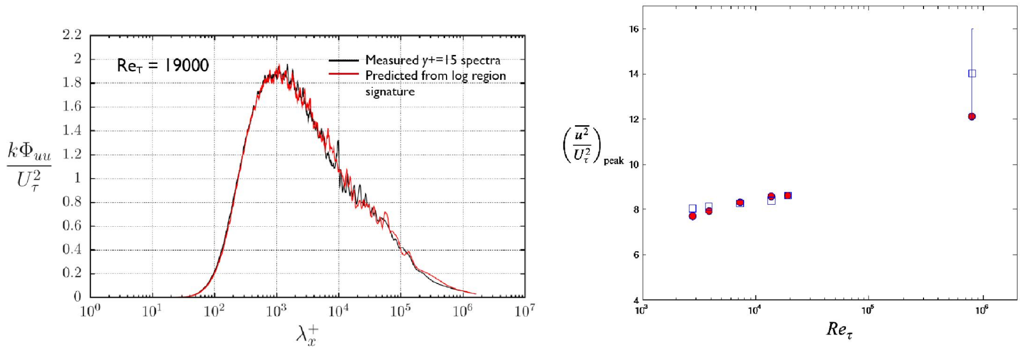

Figure 10: (a) Premultiplied spectra of the streamwise component of the velocity fluctuation in a zero pressure gradient turbulent boundary layer at high Reynolds number, together with prediction from new model that only uses the velocity signature in the log region. (b) Model predictions of turbulence intensities at $y^+ = 15$ compared with data for range of Re_τ (up to values obtained on the Utah salt-flats).

of an article for Annual Reviews on high Reynolds number wall-bounded turbulent flows (Smits et al. 2011). Furthermore, the PI has an appointment as Honorary Fellow at the University of Melbourne.

References

Abe, H., Kawamura, H. & Choi, H. 2004 Very large-scale structures and their effects on the wall shear-stress fluctuations in a turbulent channel flow up to $Re_\tau = 640$. *J. Fluids Eng.* **126**, 835–843.

Adrian, R. J. 2007 Hairpin vortex organization in wall turbulence. *Phys. Fluids* **19**, 041301.

Adrian, R. J., Meinhart, C. D. & Tomkins, C. D. 2000 Vortex organization in the outer region of the turbulent boundary layer. *J. Fluid Mech.* **422**, 1–54.

Bailey, S. C. C., Hultmark, M., Smits, A. J. & Schultz, M. P. 2008 Azimuthal structure of turbulence in high Reynolds number pipe flow. *J. Fluid Mech.* **615**, 121–138.

Bailey, S. C. C. & Smits, A. J. 2010 Experimental investigation of the structure of large- and very large-scale motions in turbulent pipe flow. *J. Fluid Mech.* **651**, 339–356.

Balakumar, B. J. & Adrian, R. J. 2007 Large- and very-large-scale motions in channel and boundary-layer flows. *Phil. Trans. R. Soc. A* **365**, 665–681.

Brown, G.L. & Thomas, A.S.W. 1977 Large structure in a turbulent boundary layer. *Phys. Fluids* **20**, 234–252.

DeGraaff, D. B. & Eaton, J. K. 2000 Reynolds-number scaling of the flat-plate turbulent boundary layer. *J. Fluid Mech.* **422**, 319–346.

Duan, L., Beekman, I. & Martín, M. P. 2010 Direct numerical simulation of hypersonic turbulent boundary layers with varying freestream mach number. *AIAA Paper 2010-0353* .

Dussauge, J.P. & Smits, A.J. 1995 Characteristic scales for energetic eddies in turbulent supersonic boundary layers. In *Proceedings of the Tenth Symposium on Turbulent Shear Flows*. Pennsylvania State University.

Fernando, E.M. & Smits, A.J. 1988 The kinematics of simple vortex loop arrays. *AIAA Paper 88-3657* .

Fernholz, H. H., Krause, E., Nockemann, M. & Schober, M. 1995 Comparative measurements in the canonical boundary layer at $Re_\theta \leq 6 \times 10^4$ on the wall of the DNW. *Phys. Fluids* **7**, 1275–1281.

Ganapathisubramani, B., Longmire, E. K. & Marusic, I. 2003 Characteristics of vortex packets in turbulent boundary layers. *J. Fluid Mech.* **478**, 35–46.

Guala, M., Hommema, S. E. & Adrian, R. J. 2006 Large-scale and very-large-scale motions in turbulent pipe flow. *J. Fluid Mech.* **554**, 521–542.

Head, M. R. & Bandyopadhyay, P. R. 1981 New aspects of turbulent boundary-layer structure. *J. Fluid Mech.* **107**, 297–337.

Hoyas, S. & Jiménez, J. 2006 Scaling of the velocity fluctuations in turbulent channels up to $Re_\tau = 2003$. *Phys. Fluids* **18**, 011702.

HUTCHINS, N., HAMBLETON, W. T. & MARUSIC, I. 2005 Inclined cross-stream stereo particle image velocimetry measurements in turbulent boundary layers. *J. Fluid Mech.* **541**, 21–54.

HUTCHINS, N. & MARUSIC, I. 2007*a* Evidence of very long meandering streamwise structures in the logarithmic region of turbulent boundary layers. *J. Fluid Mech.* **579**, 1–28.

HUTCHINS, N. & MARUSIC, I. 2007*b* Large-scale influences in near-wall turbulence. *Phil. Trans. R. Soc. Lond. A* **365**, 647–664.

JONES, M. B., MARUSIC, I. & PERRY, A. E. 2001 Evolution and structure of sink flow turbulent boundary layers. *J. Fluid Mech.* **428**, 1–27.

KIM, K. C. & ADRIAN, R. J. 1999 Very large-scale motion in the outer layer. *Phys. Fluids* **11** (2), 417–422.

KLINE, S. J., REYNOLDS, W. C., SCHRAUB, F. A. & RUNDSTADLER, P. W. 1967 The structure of turbulent boundary layers. *J. Fluid Mech.* **30**, 741–773.

KOLMOGOROV, A. N. 1941 The local structure of turbulence in incompressible viscous fluid for very large Reynolds numbers. *Dokl. Akad. Nauk SSSR* **30**, 301–305, reprinted in 1991: *Proc. R. Soc. Lond. A*, **434**, 9–13.

LIU, Z., ADRIAN, R. J. & HANRATTY, T. J. 2001 Large-scale modes of turbulent channel flow: transport and structure. *J. Fluid Mech.* **448**, 53–80.

MARUSIC, I. & KUNKEL, G. J. 2003 Streamwise turbulence intensity formulation for flat-plate boundary layers. *Phys. Fluids* **15**, 2461–2464.

MARUSIC, I., KUNKEL, G. J., ZHAO, R. & SMITS, A. J. 2004 Turbulence intensity similarity formulations for wall-bounded flows. In *Advances in Turbulence X, Proc. of the 10th European Turb. Conf.* (ed. H.I. Andersson & P.-A. Krogstad). CIMNE, Barcelona, Spain.

MARUSIC, I. & PERRY, A. E. 1995 A wall wake model for the turbulent structure of boundary layers. Part 2. Further experimental support. *J. Fluid Mech.* **298**, 389–407.

Marusic, I., Uddin, M. & Perry, A.E. 1997 Similarity law for the streamwise turbulence intensity in zero-pressure-gradient turbulent boundary layers. *Phys. Fluids* **12**, 3718–3726.

Mathis, R., Hutchins, N. & Marusic, I. 2009 Large-scale amplitude modulation of the small-scale structures in turbulent boundary layers. *J. Fluid Mech.* **628**, 311–337.

Metzger, M. M. & Klewicki, J. C. 2001 A comparative study of near-wall turbulence in high and low Reynolds number boundary layers. *Phys. Fluids* **13(3)**, 692–701.

Monty, J. P., Hutchins, N., Ng, H. C. H., Marusic, I. & Chong, M. S. 2009 A comparison of turbulent pipe, channel and boundary layer flows. *J. Fluid Mech.* **632**, 431–442.

Monty, J. P., Stewart, J. A., Williams, R. C. & Chong, M. S. 2007 Large-scale features in turbulent pipe and channel flows. *J. Fluid Mech.* **589**, 147–156.

Morrison, J. F., McKeon, B. J., Jiang, W. & Smits, A. J. 2004 Scaling of the streamwise velocity component in turbulent pipe flow. *J. Fluid Mech.* **508**, 99–131.

Nickels, T. B., Marusic, I., Hafez, S. M. & Chong, M. S. 2005 Evidence of the k^{-1} law in a high-Reynolds-number turbulent boundary layer. *Phys. Rev. Letters* **95**, 074501.

Perry, A.E. & Abell, C.J. 1977 Asymptotic similarity of turbulence structures in smooth- and rough-walled pipes. *J. Fluid Mech.* **79**, 785–799.

Perry, A. E. & Chong, M. S. 1982 On the mechanism of wall turbulence. *J. Fluid Mech.* **119**, 173–217.

Perry, A. E., Henbest, S. M. & Chong, M. S. 1986 A theoretical and experimental study of wall turbulence. *J. Fluid Mech.* **165**, 163–199.

Perry, A. E. & Li, J. D. 1990 Experimental support for the attached-eddy hypothesis in zero-pressure- gradient turbulent boundary layers. *J. Fluid Mech.* **218**, 405–438.

Perry, A. E. & Marusic, I. 1995 A wall-wake model for the turbulence structure of boundary layers. Part 1. Extension of the attached eddy hypothesis. *J. Fluid Mech.* **298**, 361–388.

Perry, A. E., Marusic, I. & Jones, M. B. 2002 On the streamwise evolution of turbulent boundary layers in arbitrary pressure gradients. *J. Fluid Mech.* **461**, 61–91.

Sahoo, D., Baumgartner, M. & Smits, A. J. 2010*a* Turbulence scaling in high mach number boundary layers. *J. Fluid Mech.* p. under review.

Sahoo, D., Desai, P. & Smits, A. J. 2010*b* Experimental investigation of helium injection in a hypersonic turbulent boundary layer. *AIAA Paper 2010-1559* .

Sahoo, D., Schultze, M. & Smits, A. J. 2009 PIV measurements in a hypersonic turbulent boundary layer with roughness. *8th International Symposium on Particle Image Velocimetry - PIV09, Melbourne, Victoria, Australia* .

Schlatter, P., Orlu, R., Li, Q., Brethouwer, G., Fransson, J. H. M., Johansson, A. V., Alfredsson, P. H. & Hennningson, D. S. 2009 Turbulent boundary layers up to $Re_\theta = 2500$ studied through simulation and experiment. *Phys. Fluids* **21**, 051702.

Smits, A.J. & Dussauge, J.-P. 2006 *Turbulent Shear Layers in Supersonic Flow*, 2nd edn. Springer Science+Business Media, Inc.

Smits, A. J. 2010 High Reynolds number wall-bounded turbulence and a proposal for a new eddy-based model. In *Notes on Numerical Fluid Mechanics and Multidisciplinary Design*. Springer.

Smits, A. J., McKeon, B. J. & Marusic, I. 2011 High Reynolds number wall turbulence. *Annu. Rev. Fluid Mech.* **43**.

Tennekes, H. & Lumley, J. L. 1972 *A First Course in Turbulence*. Cambridge, Massachusetts: The MIT Press.

Theodorsen, T. 1952 Mechanism of turbulence. In *Proc. Second Midwestern Conference on Fluid Mechanics, Mar. 17-19*. Ohio State University, Columbus, Ohio.

Tomkins, C. D. & Adrian, R. J. 2003 Spanwise structure and scale growth in turbulent boundary layers. *J. Fluid Mech.* **490**, 37–74.

Tomkins, C. D. & Adrian, R. J. 2005 Energetic spanwise modes in the logarithmic layer of a turbulent boundary layer. *J. Fluid Mech.* **545**, 141–162.

Townsend, A. A. 1976 *The Structure of Turbulent Shear Flow*. Cambridge, UK: CUP.

Tutkun, M., George, W. K., Delville, J., Stanislas, M., Johansson, P. B. V., Foucaut, J.-M. & Coudert, S. 2009 Two-point correlations in high Reynolds number flat plate turbulent boundary layers. *J. Turbul.* **10** (21), 1–23.

Zhou, J., Adrian, R. J., Balachandar, S. & Kendall, T. M. 1999 Mechanisms for generating coherent packets of hairpin vortices in channel flows. *J. Fluid Mech.* **387**, 353–396.